

# Focal mechanism estimation by classification

Ben G. Lasscock,<sup>1</sup> Brendon J. Hall,<sup>1</sup> and Michael E. Glinsky<sup>2</sup>

<sup>1</sup>*ION Geophysical, Houston, TX, USA*

<sup>2</sup>*Geotrace Technologies, Houston, TX, USA*

A classification technique for identifying focal mechanism type and fault plane orientation based on the polarity of P-wave “first motion” data is derived. A support vector machine is used to classify the polarity data in the space of spherical harmonic functions. The classification is non-parametric in the sense that there is no requirement to make *a priori* assumptions source mechanism. A metric of similarity potentially able to distinguish shear versus tensile dislocation without requiring estimation of the fault plane orientation is a natural consequence of this procedure. Going further, correlation functions between template source mechanism is derived, gives an estimate of fault plane orientation assuming a particular source mechanism.

## I. INTRODUCTION

In this article we discuss a method to robustly classify the focal mechanism of a seismic event and estimate fault plane orientation using observations of the polarity of P-wave “first motion” data. The input of this problem is a set of observations of displacement due to a seismic event across a seismic array (for microseismic monitoring) or seismic network.

Existing methods for focal mechanism classification, such as HASH<sup>1</sup> are based on a least squared optimization given a specific hypothesis of a double-couple type event. However, the least squares optimization can be unstable where the first motion polarity is misclassified. To stabilize this, the HASH algorithm implements an iterative scheme and returns the average over a set of acceptable solutions as the preferred mechanism. Where identifying acceptable solutions requires strategies for outlier rejection.

By comparison, the method we propose identifies the most likely solution for the nodal lines of these radiation patterns in a basis of spherical harmonic functions using classification. Since the spherical harmonics are the eigenfunctions of the scalar wave-equation, these solutions for the nodal lines can then be used to identify the focal mechanism of the event. As such, this approach is entirely non-parametric in the sense that we do not need to presuppose-suppose the type of focal mechanism ahead of time. One advantage of this approach is that it admits a natural metric of similarity between the focal mechanism types (e.g. double couple, CLVD) without requiring an estimate of source type or fault plane orientation. A procedure for computing the correlation between template focal mechanisms types and the non-parametric estimate is derived, along with a corresponding estimate of the fault plane orientation.

Finally, we show that the performance of the classification approach compared to HASH using the Northridge data-set supplied with the HASH software<sup>2</sup>.

## II. MATHEMATICAL FOUNDATIONS

It is well known complex seismic sources can be represented by systems of force couples<sup>3,4</sup> and that angu-

lar variation of the displacement due to a seismic event can be used to characterize the source mechanism and its orientation. We limit our analysis to the simplified case of a compressional (or P-wave) arrival in a homogeneous isotropic media. Our approach will be to encode the angular dependence of the displacement in the basis of spherical harmonics. It will be shown that by working in this basis, event classification (e.g. shear versus tensile failure) and estimation of the fault plane orientation is mathematically convenient.

Physically, the spherical harmonic functions are also eigenfunctions of the scalar wave-equation. Solutions to the angular dependence of the P- and S-wave radiation patterns are tabulated in Ben-Menahem and Singh<sup>4</sup>. Given a particular orientation of the fault plane, the angular dependence of displacement due to standard focal mechanisms such as the double couple and clvd sources are also known in this basis. As such we can relate solutions to the scalar wave equation, to particular source mechanism.

But more generally, any square-integrable function, defined on the 2-sphere, can be expressed in terms of the orthonormal basis:

$$f(\vec{x}) = \sum_{l=0}^{\infty} \sum_{m=-l}^l \hat{f}_{lm} Y_{lm}(\theta, \phi), \quad (1)$$

where  $Y_{lm}(\theta, \phi)$  are the spherical harmonic functions of azimuth  $\phi$  and inclination  $\theta$ , and  $\hat{f}_{lm}$  are complex coefficients. The variable indices by  $l$ - and  $m$ -respectively are commonly referred to as the degree and order of the basis function. It is also common to refer to each degree  $l = 0, 1, 2$  as the monopoles, dipole and quadrupole terms (in deference to the multipole expansion of electrostatics). Where this series has good convergence properties, we can view this expansion as a kind of data compression, in the sense that a compact set of coefficients  $\hat{f}_{lm}$  provides a concise description of the function. An important mathematical property of this expansion is that the norm of the coefficients in the span of each degree are rotationally invariant. As such a metric for distinguishing the type of seismic event, for example shear-failure versus tensile dislocation, exist without knowledge of the orientation of the respective fault planes. Template solutions for common focal mechanisms, given a particular

orientation, are known in this basis in Table II. This table provides a theoretical template in terms of the relative weighting of basis functions for common seismic events. With more general solutions tabulated in Ben-Menahem and Singh<sup>4</sup>. Hence the basis of spherical harmonics, at least in the isotropic media, diagonalizes the problem of characterizing standard seismic source mechanisms.

### A. Kernel methods

In this section, we will show how modern techniques of classification taken from the discipline of machine learning can be applied to earthquake seismology.

Conditional on a set of event picks of a P-wave arrival and a velocity model, we can describe the inputs our problem as the set  $\{\vec{x}_i, y_i\}$  of coordinates on a unit sphere (parameterized by a azimuth and take-off angle) and the sign of the first motion of an incident 'P-wave' seismic signal. The input data  $y_i$  is from one of two classes, positive first motion polarity, or negative first motion polarity. From this set of inputs our goal is to estimate the nodal lines of the radiation pattern.

Since the data is imperfect, it is expected that there maybe mis-classification error. As such we need a classification algorithm that is robust to a degree of mis-classification of the first motion. Further, we require a classification algorithm that is tractable on the surface of a sphere and provides a convenient measure of uncertainty.

The support vector machine<sup>5</sup> solves for the maximum separating hyper-plane (nodal lines) between linearly separable classes of data, with the width of the hyper-plane providing a natural metric of uncertainty. Soft thresholding extensions of this support vector machine<sup>5</sup> provides robustness to mis-classification. We elaborate further on the support vector classifier in Appendix A. Based on a set of input training data, the support vector machine learns the function:

$$f(\vec{x}) = \sum_{i=1}^N \alpha_i y_i k(\vec{x}, \vec{x}_i) + \beta_0, \quad (2)$$

by constrained optimization. Here,  $y_i$  is the polarity of the  $i^{th}$  arrival, the coefficients  $\alpha_i$  are Lagrange multipliers that are solved for, an output of the algorithm,  $\beta_0$  is a constant and  $k(\vec{x}, \vec{x}_i)$  is a kernel. Domains in the input space are defined by the sign of the function  $f(\vec{x})$ , i.e. the solution  $f(\vec{x})$  parameterizes the nodal lines. The kernel function  $k(\vec{x}, \vec{x}_i)$  can be thought of as a generating functional projecting the classifier into a higher dimensional feature space. The so-called class of dot-product kernels are appropriate for classification on a sphere. We will show that a particular kernel:

$$k(\vec{x}, \vec{x}_i) = (\langle \vec{x}, \vec{x}_i \rangle + 1)^d. \quad (3)$$

projects into a basis of spherical harmonic functions, truncating at degree- $d$ .

Expanding the kernel in Eq. (3) in a basis of Legendre polynomials  $P_l$ :

$$f(\vec{x}) = \sum_{i=1}^N \alpha_i y_i \sum_{l=1}^{\infty} a_l P_l(\langle \vec{x}, \vec{x}_i \rangle), \quad (4)$$

where the coefficients of the expansion are:

$$a_l = \int_{-1}^1 dx (x+1)^d P_l(x). \quad (5)$$

This integral evaluates to<sup>5</sup>:

$$a_l = \begin{cases} \frac{2^{d+1} \Gamma(d+1)}{\Gamma(d+2+l) \Gamma(d+1-l)} + \frac{1}{2} \sqrt{\frac{1}{\pi}} \beta_0 \delta_{l0} & \text{if } l \leq d \\ 0 & \text{otherwise} \end{cases},$$

here we have absorbed the constant term into the coefficient for  $l = 0$ . Hence the parameter  $d$  in the definition of the kernel truncates the expansion in Legendre polynomials at degree  $d$ , which is a useful feature. To formulate an expression in terms of the spherical harmonic functions we use the addition theorem:

$$\begin{aligned} P_l(\langle \vec{x}, \vec{x}_i \rangle) &= \sum_{m=-l}^l Y_{lm}^*(\theta', \psi') Y_{lm}(\theta, \psi) \\ f(\vec{x}) &= \sum_{i=1}^N \alpha_i y_i \sum_{l=1}^{\infty} a_l \frac{4\pi}{2l+1} \times \\ &\quad \sum_{m=-l}^l Y_{lm}^*(\theta', \psi') Y_{lm}(\theta, \psi), \end{aligned} \quad (6)$$

where  $Y_{lm}^*$  notation denotes the complex conjugate of the spherical harmonic function. Collecting terms:

$$\begin{aligned} f(\vec{x}) &= \sum_{l=1}^{\infty} \sum_{m=-l}^l \hat{f}_{lm} Y_{lm}(\theta, \psi) \\ \hat{f}_{lm} &= \frac{4\pi}{2l+1} \sum_{i=1}^N \alpha_i y_i a_l Y_{lm}^*(\theta', \psi'), \end{aligned} \quad (7)$$

each of these coefficients maps the separating margin onto the basis of spherical harmonics, from which we can assign physical meaning.

### B. Assumptions of symmetry

Physically, seismic events such as earthquakes can be modeled as a closed system. As such conservation of momentum, and angular momentum can be enforced. For the problem of earthquake classification, assuming an isotropic media, this is equivalent to the requirement that the solution be even under parity transformation. To ensure that this is the case we map observations from the upper to lower half spheres (and vice versa) to ensure that the optimal non-parametric solutions respect this symmetry.

### C. Mapping the kernel estimation to a parsimonious solution

The kernel estimation of the nodal lines is entirely driven by the data. However, analysts require a mapping onto a set of parsimonious solutions from which they can interpret physical meaning. In this section we derive a rotationally invariant signature of a seismic event based on its multipole expansion. We will then go on to develop formalism for estimating correlation functions between events with a nested optimization over the fault plane orientation.

Seismic sources characterized as systems of force couples are orientated with respect to the normal of a planar fault and the direction of the slip. Particular solutions for the angular dependence can be derived given a particular orientation<sup>4</sup>; template solutions for standard seismic sources are tabulated in Table II. A signature of the seismic event can be expressed in terms of the norm of the coefficients at each order:

$$q_l = \sum_{m=-l}^l \hat{f}_{lm}^* \hat{f}_{lm}, \quad (8)$$

where each  $q_l$  tells us the relative contribution of monopole, dipole, quadrupole, etc. composition of the source. In Appendix B we show that this signature is invariant under rotations.

Going further, we can define a correlation function between seismic events as:

$$\langle g, f \rangle = \int d^3x g^*(R(\alpha, \beta, \gamma) \cdot \vec{x}) f(\vec{x}) \quad (9)$$

where  $R(\alpha, \beta, \gamma)$  is a rotation matrix parameterized by the Euler angles. The role of the rotation matrix in the correlation function is to recognize that the relative orientation of the focal plane between the two events maybe different. The action of the rotation applied in the input space generates a rotation in the feature space. The set of matrices that perform this rotation in the feature space of spherical harmonics are called Wigner's D matrices, see Morrison and Parker<sup>6</sup> for review. In Appendix B we show that we can write the rotation of the estimated nodal lines as:

$$f(R(\alpha, \beta, \gamma) \cdot \vec{x}) = \sum_{l=0}^{\infty} \sum_{m,n=-l}^l D_{mn}^l(\alpha, \beta, \gamma) \hat{f}_{ln} Y_{lm}(\theta, \phi).$$

Using the orthogonality condition of the spherical harmonics leads to a discrete expression for the correlation function:

$$\langle g, f \rangle = \sum_{l=0}^{\infty} \sum_{m,n=-l}^l D_{mn}^{l*}(\alpha, \beta, \gamma) \hat{g}_{ln}^* \hat{f}_{lm}, \quad (10)$$

where we have made use of the fact that the D-matrices do not mix coefficients of different degree. By optimizing the correlation function over the Euler angles we obtain the correlation between and two source mechanisms, and corresponding orientation of the fault plane. Details of the optimization algorithm can be found in Appendix B.

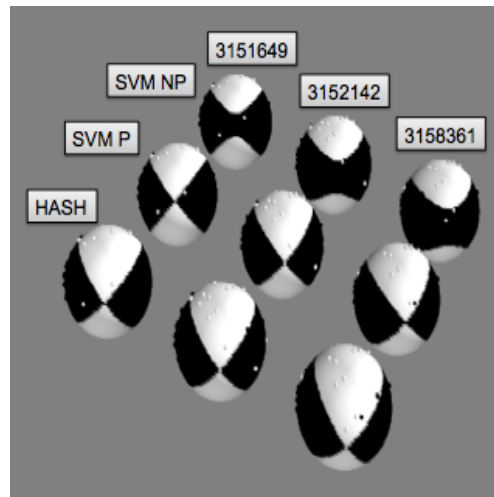


FIG. 1. Shows the HASH (front row), (P) parametric SVM equivalent solution (middle row) and (NP) non-parametric solution (back row). The catalog event ids are 3151649, 3152142 and 3158361.

### III. APPLICATION TO NORTHRIDGE DATA

In this section we apply the support vector classifier to the Northridge dataset supplied with the USGS HASH software<sup>7</sup>. The HASH algorithm<sup>2</sup> provides focal mechanism classification using first motion polarity based on least squares, and is considered to be robust.

The example dataset north1 from Hardebeck and Shearer<sup>2</sup> is analyzed by HASH and the support vector classifier. The default parameterization of HASH is used, except that we extend the number of iterations to from 30 to 3000. The north1 dataset contains the azimuth, take-off angles and first arrival polarity for a collection of earthquakes from the Northridge region of California, recorded by the Southern California Seismic Network. Polarity reversals are applied where appropriate, see the HASH manual<sup>2</sup>.

In Fig. 1 we show a graphical example of focal mechanism solutions derived from HASH compared to the parametric and non-parametric estimates derived from the classifier. Like HASH, the parametric-solution assumes *a priori* a double-couple (shear) event. Given this template for the event in the basis of spherical harmonic functions Table II, the fault plane orientation is estimated using Eq. (10). Whereas the non-parametric solution is simply the superposition derived from Eq. (1) (without assuming a particular type of mechanism or solving for the fault plane orientation).

Extending the analysis to the entire Northridge (north1) dataset, in Table I, we evaluate the respective algorithms by their overall rate of mis-classification.

TABLE I. The average rate of misclassification for the Northridge (north1) dataset. The parametric and non-parametric classifiers are compared to the HASH algorithm.

svm parametric	svm non-parametric	HASH
15.5%	14.7%	15.3%

#### IV. CONCLUSIONS

We presented a new technique for classifying the focal mechanism classification using P-wave first motion polarity data. This new approach provides classification for a general set of sources including combinations of shear- and tensile failure (double couple and CLVD). Robustness to misclassification error is achieved using soft thresholding, rather employing importance weighting observations or by heuristic outlier rejection. This suits the problem at hand where the observations along the nodal lines are the most informative, but also the most likely to be misclassified. We also derive a rotationally invariant source signature that may provide comparison between seismic events without requiring a parameterization of the source type or fault plane orientation. This signature has applications for distinguishing shear- from tensile failure, or comparing linear combinations of both.

Finally we compare the performance of the classifier to the Northridge data-set supplied with HASH<sup>2</sup> and performs as well as the current state of the art.

#### Appendix A: The support vector classifier

In this section we provide a short overview of the support vector classifier. We follow Hastie, Tibshirani, and Friedman<sup>8</sup> and Scholkopf and Smola<sup>5</sup> as references. The software implementation of the support vector classifier used in this report sklearn version 0.14<sup>9</sup>.

First motion polarity on a 2-sphere is not linearly separable in a rectangular coordinate system, therefore the strategy of the support vector machine is to linearize the problem by expanding into a higher dimensional space. The space where the observations are made is commonly referred to as the input space, the space where the classification is performed called the feature space. The efficiency of the support vector machine is subtended by the so-called kernel trick, which allows this expansion to into feature space to be carried out in terms of inner products calculated in the input space.

Using the notation from Sec. II A each datum is described a Cartesian coordinate and a class ( $\{\vec{x}_i, y_i\}$ ), where the the class  $y_i$  is the first motion polarity. Consider the example where we have  $N$  observations of the first motion polarity over the surface of a unit sphere. Suppose that there is some mapping  $\vec{\phi}(\vec{x})$  into a higher dimensional space where this can be considered as a linear problem. That is, where there exists some hyper-plane

separates the two classes:

$$f(\vec{x}) = \langle \vec{\beta}, \vec{\phi}(\vec{x}) \rangle + \beta_0. \quad (\text{A1})$$

The strategy the support vector classifier uses is to optimize the width of a margin separating classes in this domain, which can be written as the optimization:

$$\min_{\vec{\beta}, \vec{\eta}} \frac{1}{2} \|\beta^2\| + C \sum_{i=1}^N \eta_i, \quad (\text{A2})$$

subject to the constraints:

$$y_i (\langle \vec{\beta}, \vec{\phi}(\vec{x}_i) \rangle + \beta_0) \geq 1 - \eta_i \\ \eta_i \geq 0, \quad i = 1, \dots, N. \quad (\text{A3})$$

The addition of a set of slack variables  $\eta_i$  stabilizes the algorithm by allowing for for mis-classification, but with a penalty. The penalty leads the optimization to prefer mis-classification close to the nodal line, which it is expected to be most prevalent.

This makes the algorithm robust where the data is not exactly separable in the space spanned by  $\vec{\phi}$ , a problem which will be caused by mis-classification of the first motion polarity.

The optimization described above is problem of quadratic programming, which is solved by introducing a set of Lagrange multipliers  $\alpha_i$  for each constraint. The so-called dual form of the Lagrangian is:

$$\mathcal{L} = \sum_{i=1}^N \alpha_i - \frac{1}{2} \sum_{i,j=1}^N \alpha_i y_i \alpha_j y_j \langle \vec{\phi}(\vec{x}_i), \vec{\phi}(\vec{x}_j) \rangle. \quad (\text{A4})$$

For a certain class of function  $\vec{\phi}(\vec{x})$ , the inner product (called a kernel) maybe evaluated in the input space directly. As an example, we show that the inner product kernel Eq. (3) maps to an expansion in spherical harmonic functions, a natural basis for our problem. For a separable dataset, the Lagrange multipliers are non-zero only for points along the optimal separating hyper-plane. The coordinates of the corresponding data are called support vectors.

#### Appendix B: Optimization for estimating fault plane orientation

In Sec. II A we have established that a set of nodal lines along a unit sphere can be expressed as a series of spherical harmonic functions:

$$f(\vec{x}) = \sum_{l=0}^{\infty} \sum_{m=-l}^l \hat{f}_{lm} Y_{lm}(\theta, \phi). \quad (\text{B1})$$

Were we to perform a rotation of this coordinate system, the same general expression must still hold, and the norm of the coefficients must be invariant, however the individual coefficients themselves may change. An irreducible representation of the rotations group in the span

of spherical harmonic functions is given by the Wigner-D matrix. That is, for some rotation  $R(\alpha, \beta, \gamma)$ :

$$f(R \cdot \vec{x}) = \sum_{l=0}^{\infty} \sum_{m=-l}^l D_{mm'}^l \hat{f}_{lm'} Y_{lm}(\theta, \phi). \quad (\text{B2})$$

The properties of this representation of rotations is that it is unitary and irreducible in the span of the harmonic functions at each order. These properties ensure that the norm of the coefficients of the expansion, at each degree in the basis of harmonic functions is invariant under rotations:

$$\begin{aligned} q_l &= \sum_{m=-l}^l \hat{f}_{lm}^* \hat{f}_{lm} \\ &\rightarrow \sum_{m, m'=-l}^l \hat{f}_{lm}^* D_{mm'}^{l*} D_{m'm}^l \hat{f}_{lm} \\ &= \sum_{mm'=-l}^l \hat{f}_{lm}^* \delta_{m'm} \hat{f}_{lm} \\ &= q_l. \end{aligned} \quad (\text{B3})$$

An explicit form of Wigner-D matrices is:

$$D_{mn}^l(\alpha, \beta, \gamma) = e^{-im\alpha} d_{mn}^l(\beta) e^{-in\gamma}, \quad (\text{B4})$$

where the so-call ‘‘little Wigner-d’’ matrix is purely real. We use the formulation of Morrison and Parker<sup>6</sup> for the Wigner-D matrices, except for an overall sign difference in the  $d_{10}^2$  term.

Next we apply these rotation matrices to optimize the correlation function in Eq. (10). The discrete form of the correlation function is derived by using the orthogonality condition (suppressing the argument  $\alpha, \beta$  and  $\gamma$ ):

$$\begin{aligned} \langle g, f \rangle &= \int d^3x g^*(R\vec{x}) f(\vec{x}) \\ &= \sum_{l, l'=0}^{\infty} \sum_{n, m'} \int d\Omega D_{m'n}^{l*} \hat{g}_{l'n}^* \hat{f}_{lm} Y_{l'm'}^* Y_{lm} \\ &= \sum_{l, l'=0}^{\infty} \sum_{m, m', n} D_{m'n}^{l*} \hat{g}_{l'n}^* \hat{f}_{lm} \delta_{l'l} \delta_{m'm'} \\ &= \sum_{l=0}^{\infty} \sum_{m, n} D_{mn}^{l*} \hat{g}_{ln}^* \hat{f}_{lm}. \end{aligned}$$

The optimization with respect to the variables  $\alpha, \beta$  and  $\gamma$  is performed numerically.

### Appendix C: Seismic source templates

In this section we provide a lookup table of theoretical templates of the compression mode of the displacement oriented radially, for standard seismic sources in a homogeneous isotropic media. Solutions in terms of the Hansen vectors are taken from Table 4.4 of Ben-Menahem and Singh<sup>4</sup>. The solutions for the first arrival are given

TABLE II. Describes the angular variation of the radial component of displacement in terms of spherical harmonic functions. The source templates summarized are double couple (D.C.), tensile dislocation (Tensile) and tangential dislocation (Tangential). The brackets  $(\cdot, \cdot)$  define the template direction of the fault normal and direction of slip in rectangular coordinates. For the tensile dislocation (CLVD sources) the constant  $\alpha = 2 + 3\frac{\lambda}{\mu}$ , where  $\lambda$  and  $\mu$  are the first Lamé parameter and the shear modulus respectively.

Source	(Fault normal/slip)	Template
D.C.	(31) + (13)	$-i(Y_{12} + Y_{-12})$
Tensile	(3)	$\alpha Y_{00} + 4\sqrt{5}Y_{02}$
Tangential	(3)	$Y_{02} - \frac{i}{2}(Y_{22} + Y_{-22})$ .

in terms of the Hansen vector  $\vec{L}$  (in spherical polar coordinates) of the form:

$$\vec{L}_{lm}(r, \theta, \phi) = \vec{\nabla} h_l^2(r) \tilde{Y}_{lm}(\theta, \phi), \quad (\text{C1})$$

where  $h_l^2(r)$  is the spherical Hankel functions of a second kind. The amplitudes of the first break are required to be measured radially, the projection of the Hansen vector radially is:

$$\hat{r} \cdot \vec{L}_{lm}(r, \theta, \phi) = \frac{\partial}{\partial r} h_l^2(r) \tilde{Y}_{lm}(\theta, \phi), \quad (\text{C2})$$

where  $\hat{r}$  is the radial unit vector. Asymptotically, the Hankel functions tend to Morse and Feshbach<sup>10</sup>:

$$h_l^2(x) = \frac{1}{x} (i)^{l+1} e^{-ix}, \quad (\text{C3})$$

which introduces a relative sign when collecting terms of degree 0 and 2.

We also note that the normalization of the spherical harmonics used in Ben-Menahem and Singh<sup>4</sup>, to our definition:

$$\tilde{Y}_{lm}(\theta, \phi) = (-1)^m \sqrt{\frac{4\pi(l+m)!}{(2l+1)(l-m)!}} Y_{lm}(\theta, \phi). \quad (\text{C4})$$

With these adjustments, the amplitudes (up to an overall constant) for a common set of source mechanism, in terms of the spherical harmonics, are given in Table II. The  $(\cdot\cdot)$  notation in this table labels the orientation of the fault normal and direction of slip respectively.

<sup>1</sup>J. L. Hardebeck and P. M. Shearer, Bulletin of the Seismological Society of America **92**, 2264 (2002).

<sup>2</sup>J. L. Hardebeck and P. M. Shearer, ‘‘HASH: A fortran program for computing earthquake first-motion focal mechanisms v1.2 january 31, 2008,’’ <http://earthquake.usgs.gov/research/software/index.php> (2008).

<sup>3</sup>K. Aki and P. G. Richards, *Quantitative seismology* (University Science Books, 2002).

<sup>4</sup>A. Ben-Menahem and S. J. Singh, *Seismic waves and sources* (Springer Verlag New York, 1981).

<sup>5</sup>B. Scholkopf and A. Smola, *Learning with Kernels* (The MIT Press, 2002).

<sup>6</sup>M. A. Morrison and G. A. Parker, Australian Journal of Physics **40**, 465 (1987).

<sup>7</sup><http://earthquake.usgs.gov/research/software/index.php>.

<sup>8</sup>T. Hastie, R. Tibshirani, and J. Friedman, *Elements of Statistical Learning* (Springer-Verlag, 2001).

<sup>9</sup><http://scikit-learn.org>.

<sup>10</sup>M. Morse and F. Feshbach, *Methods of theoretical physics* (Feshbach Publishing LLC, 1953).